

Intrinsic Control of Precise Dendritic Targeting by an Ensemble of Transcription Factors

Takaki Komiyama^{1,2} and Liqun Luo^{1,*}

¹Howard Hughes Medical Institute
Department of Biological Sciences
Neurosciences Program
Stanford University
Stanford, California 94305

Summary

Proper information processing in neural circuits requires establishment of specific connections between pre- and postsynaptic neurons. Targeting specificity of neurons is instructed by cell-surface receptors on the growth cones of axons and dendrites, which confer responses to external guidance cues [1, 2]. Expression of cell-surface receptors is in turn regulated by neuron-intrinsic transcriptional programs. In the *Drosophila* olfactory system, each projection neuron (PN) achieves precise dendritic targeting to one of 50 glomeruli in the antennal lobe [3]. PN dendritic targeting is specified by lineage and birth order [4], and their initial targeting occurs prior to contact with axons of their presynaptic partners, olfactory receptor neurons [5]. We search for transcription factors (TFs) that control PN-intrinsic mechanisms of dendritic targeting. We previously identified two POU-domain TFs, *acj6* and *drifter*, as essential players [6]. After testing 13 additional candidates, we identified four TFs (LIM-homeodomain TFs *islet* and *lim1*, the homeodomain TF *cut*, and the zinc-finger TF *squeeze*) and the LIM cofactor *Chip* that are required for PN dendritic targeting. These results begin to provide insights into the global strategy of how an ensemble of TFs regulates wiring specificity of a large number of neurons constituting a neural circuit.

Results

For technical simplicity, we studied larval born GH146-Gal4-positive PNs, originating from three neuroblast lineages, anterodorsal (adPNs), lateral (IPNs), and ventral (vPNs). Out of ~25 classes defined by their glomerular targets, we focused on 17 classes (see last figure for summary) whose target glomeruli are reliably recognized across different animals. The MARCM technique [7] allows us to visualize and genetically manipulate PNs in neuroblast (Figures 1–3) and single-cell (Figure 4) clones in otherwise heterozygous animals, so we can study PN-intrinsic programs for dendritic targeting. GH146 is expressed only in postmitotic PNs (J. Liu, M. Spletter, and L.L., unpublished observation).

We previously identified *acj6* and *drifter* as lineage-specific regulators of PN dendritic targeting [6]. To identify additional transcription factors (TFs) that regulate dendritic targeting of different PN classes, we tested candidates that have been shown to regulate neuronal subtype specification and targeting specificity and have available loss-of-function mutants. We tested (1) the expression of candidate genes in PNs at 18 hr after puparium formation (APF) when PN dendrites are in the process of completing their initial targeting, and/or (2) their requirement in PNs by examining dendritic targeting in homozygous mutant MARCM clones.

In addition to the eight genes described below, we examined five other TFs that were not pursued because of the lack of expression in GH146-PNs at 18 hr APF (*aristaleless* and *pdm-1*) or the lack of targeting defects in homozygous mutant PNs (*abrupt* [*ab*^{K02807}], *kruppel* [*Kr*¹], and *Dichaete* [*Dichaete*⁸⁷]). Experiments on the zinc-finger TF *squeeze* are described in Figure S1 in the Supplemental Data available online.

LIM-HD Factors and PN Targeting

LIM-homeodomain (LIM-HD) TFs are involved in multiple events during neuronal development [8, 9]. Most functions of LIM-HD factors require the LIM domain-binding cofactor [9], which is represented in *Drosophila* by ubiquitously expressed *Chip* [10, 11]. *Chip* antibody [10] revealed ubiquitous expression of *Chip* in cells around the antennal lobe (AL) including all GH146-PNs at 18 hr APF (Figure 1A).

We tested the requirement of *Chip* in PN dendritic targeting. Wild-type adPNs, IPNs, and vPNs target stereotyped sets of glomeruli (Figures 1D₁–1D₃) [4, 12]. PNs homozygous for a *Chip* null allele (*Chip*^{es.5}) failed to target most of the correct glomeruli (Figures 1E₁–1E₃, quantified in Figure 4A) and occupied inappropriate glomeruli (data not shown). Most adPN and IPN clones (12/13) also mistargeted a fraction of dendrites to the structure ventral to the AL, the suboesophageal ganglion (SOG) (data not shown). Thus, *Chip* is required for targeting specificity of most, if not all, PN classes studied here, and *Chip*-interacting proteins including LIM-HD factors likely play important roles in PN dendritic targeting.

Five LIM-HD factors have been characterized in *Drosophila*: *apterous*, *arrowhead*, *islet*, *lim1*, and *lim3*. We did not pursue *apterous*, *arrowhead*, or *lim3* because they are not expressed in GH146-PNs at 18 hr APF (*apterous*) or they do not have targeting defects in PNs homozygous for null alleles (*lim3*^{37Bd6} and *awh*¹⁶).

Islet antibody [13] detected *Islet* expression in ~50% adPNs and most IPNs but not in vPNs at 18 hr APF (data not shown) and adult (Figure 1B). *islet*^{-/-} adPNs failed to target many (but not all) of the normal target glomeruli, including VA1Im, VA3, and VM7 (Figures 1F₁ and 4A). In addition, DA1, a IPN target, was often specifically mistargeted (Figure 1F₁). Defects of *islet*^{-/-} IPNs were very similar to *Chip*^{-/-} IPN defects (Figures 1F₂ and 4A). A fraction of dendrites often mistargeted to the SOG.

*Correspondence: lluo@stanford.edu

²Present address: Janelia Farm Research Campus, Howard Hughes Medical Institute, Ashburn, Virginia 20147.

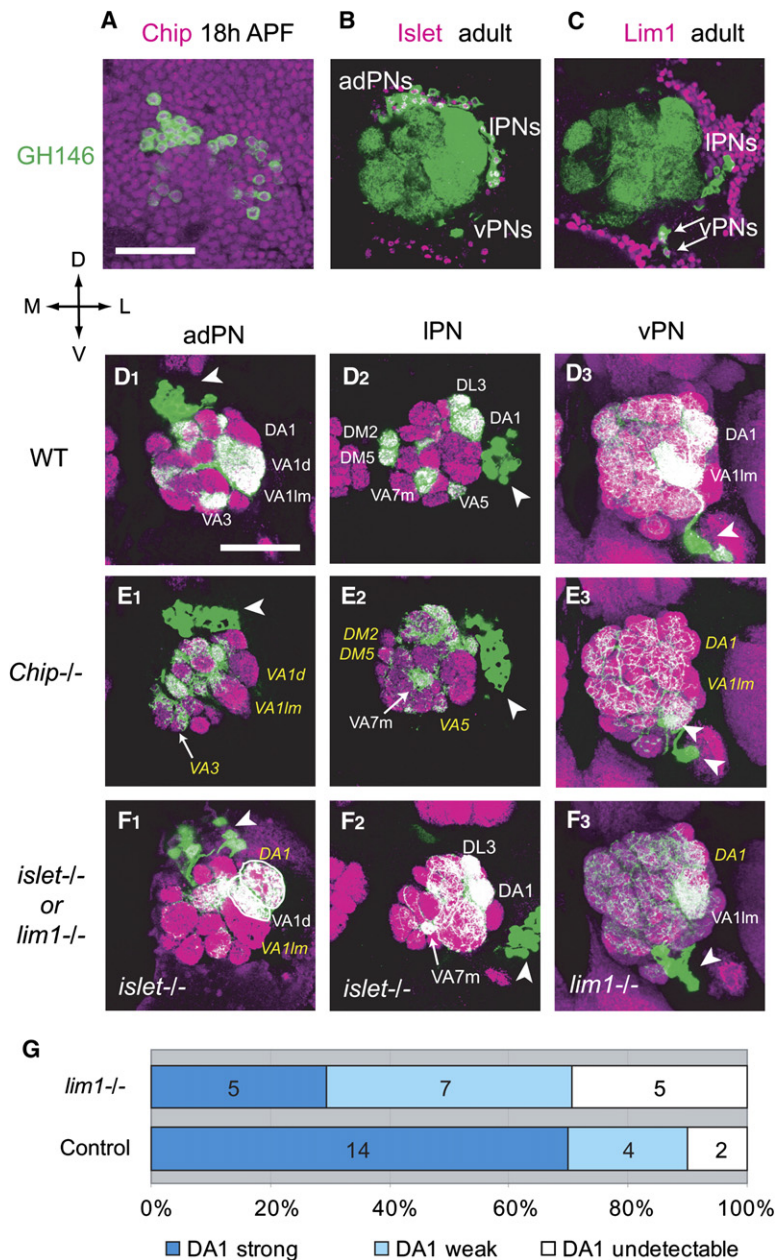


Figure 1. *Chip*, *islet*, and *lim1* Are Required for PN Dendritic Targeting

(A–C) *Chip* is expressed ubiquitously in the central brain at 18 hr after puparium formation (APF) (A). *Islet* is expressed in about half of adPNs and a majority of IPNs in adult (B). *Lim1* is expressed in vPNs, but not in IPNs or adPNs (C). Magenta: anti-*Chip*, anti-*islet*, or anti-*Lim1*; green: UAS-mCD8GFP driven by GH146-Gal4. A single confocal section is shown. D, dorsal; V, ventral; L, lateral; M, medial.

(D) Wild-type adPNs, IPNs, and vPNs target stereotypical sets of glomeruli. Single confocal sections (D_{1,2}) or confocal z-projections (D₃) are shown. Single confocal sections represent a small part of the AL, and thus the AL appears smaller.

(E) *Chip*^{-/-} adPNs, IPNs, and vPNs exhibit severe dendritic targeting defects, with little specific targeting to defined glomeruli.

(F) *islet*^{-/-} adPNs fail to target many glomeruli, including VA1Im, and have incorrect innervation to a IPN glomerulus DA1 (F₁). *islet*^{-/-} IPNs fail to target many glomeruli, except DA1 and DL3 (and occasionally VA7m) (F₂). *lim1*^{-/-} vPNs fail to have dense innervation of DA1 (F₃).

(G) Quantification of the frequency of the *lim1*^{-/-} DA1 vPN phenotype. Compared to wild-type, *lim1*^{-/-} vPNs more often fail to have strong innervation of DA1. Numbers in the graph indicate numbers of samples.

Unless otherwise noted, in this and all subsequent figures, the right hemisphere is shown with dorsal (D) to the top and lateral (L) to the right as indicated (V, ventral; M, medial). Green is mCD8-GFP marking MARCM clones, and magenta is the synaptic marker nc82. All scale bars represent 50 μm. Arrowheads indicate PN cell bodies. White labels indicate glomeruli whose targeting is normal, and yellow italic labels indicate glomeruli whose targeting is defective.

Within the AL, dendrites were diffusely spread, although DA1 and DL3 were always correctly innervated. Targeting of *islet*^{-/-} vPNs was normal (n = 16), consistent with their lack of *Islet* expression (data not shown).

Lim1 antibody [14] revealed *Lim1* expression in most or all vPNs, but not in adPNs or IPNs in adults (Figure 1C). The expression pattern appears similar at 18 hr APF (data not shown), although vPNs are difficult to identify unambiguously at early stages. *lim1*^{-/-} adPNs showed no defects, consistent with the lack of *Lim1* expression. *lim1*^{-/-} IPNs rarely showed a cell number decrease (n = 2/14), but in clones in which the cell number was normal, *lim1*^{-/-} IPNs targeted correct glomeruli (data not shown). In contrast, *lim1*^{-/-} vPNs showed a specific targeting defect. Wild-type vPNs innervate DA1 and VA1Im densely because of the single vPNs that specifically innervate these glomeruli, in

addition to the diffuse innervation all over the AL contributed by the pan-AL vPN (Figure 1D₃) [12]. In *lim1*^{-/-} vPNs, DA1 innervation was greatly reduced and sometimes undetectable (Figure 1F₃, quantified in Figure 1G). Therefore, *lim1* is required for dendritic targeting by a single vPN class, vDA1, despite its general expression in vPNs. *lim1* might be redundant with other factors in non-DA1 vPNs, as supported below.

We note that phenotypes of *islet* and *lim1* combined are only a subset of the *Chip* phenotype (Figure 4A). Additional *Chip* phenotype may be explained by non-*Lim*-HD molecules interacting with *Chip* [15–17].

cut Is Required for Targeting of Several IPN and All vPN Classes

cut encodes a homeodomain TF that regulates sensory organ identity [18] and dendritic morphogenesis

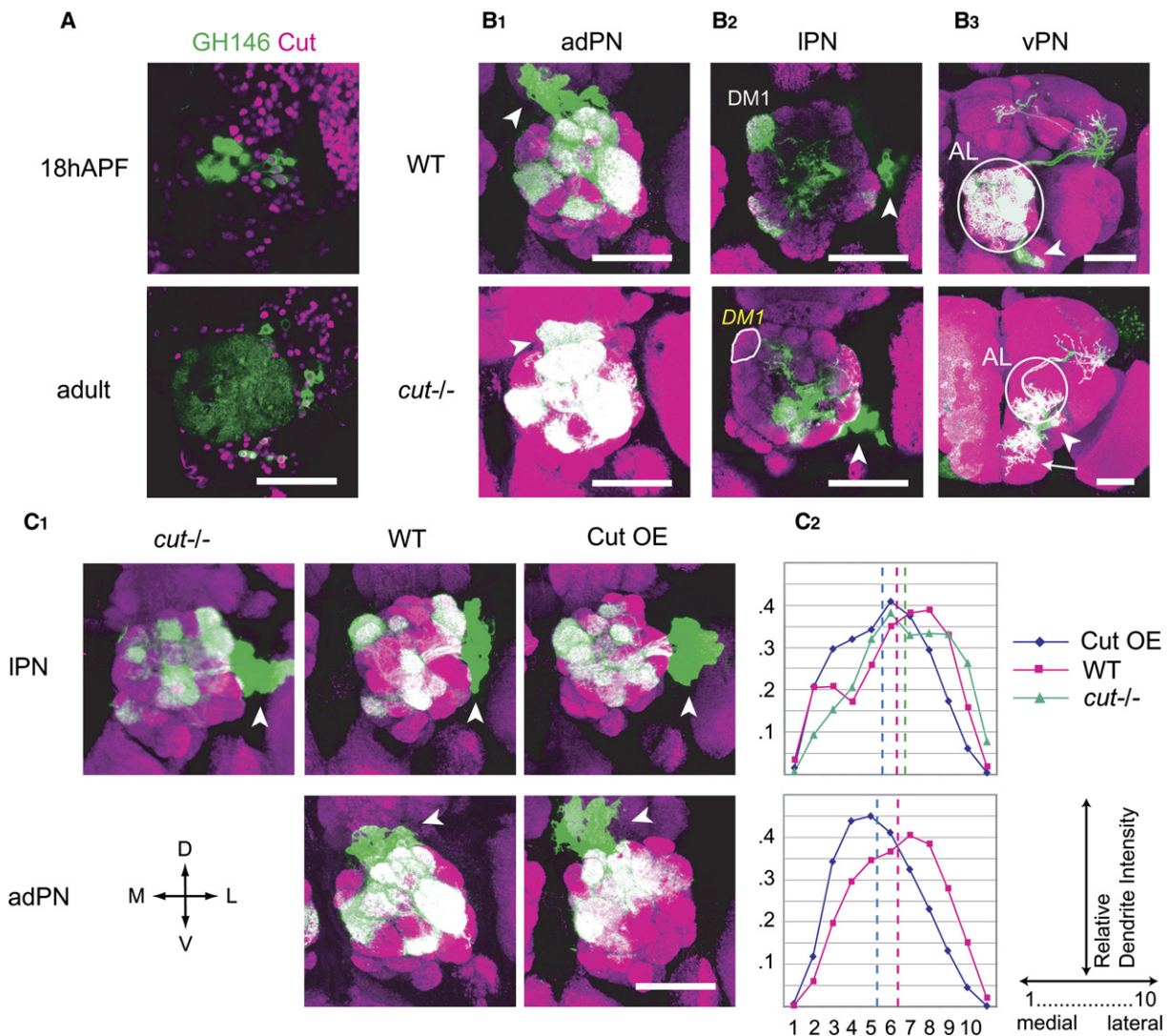


Figure 2. *cut* Is Required for Dendritic Targeting by a Specific Subset of PN Classes

(A) *Cut* is expressed in ~8 adPNs (likely embryonically born and not characterized in this study, see text), ~8 IPNs, and all vPNs in adults. A similar pattern was observed at 18 hr APF. Magenta, anti-*Cut*; green, UAS-mCD8GFP driven by GH146-Gal4. Single confocal sections are shown. (B) $cut^{-/-}$ adPNs target normally, but $cut^{-/-}$ IPNs fail to target DM1. $cut^{-/-}$ vPNs have severe targeting defects, with a large fraction of dendrites targeting the SOG (arrow) and often completely missing the AL (circle). See Figure 3E for quantification. Partial (IPN) or full (adPN and vPN) confocal z-projections are shown.

(C₁) Dendrites of $cut^{-/-}$ IPNs shift laterally, while dendrites of IPNs and adPNs overexpressing *Cut* (*Cut* OE) shift medially, compared to wild-type IPNs and adPNs, whose dendrites are rather evenly distributed along the medial to lateral axis. The cell number did not appear to be altered in these genetic manipulations. D, dorsal; M, medial; V, ventral; L, lateral.

(C₂) Quantitative analysis of dendritic distributions along the medial-lateral axis. The mean of mean positions from multiple brains for IPN WT, 5.74 ± 0.09 (n = 8); IPN $cut^{-/-}$, 5.26 ± 0.07 (n = 12); IPN *Cut*OE (overexpression), 6.41 ± 0.15 (n = 11); adPN WT, 5.62 ± 0.06 (n = 25); adPN OE, 6.60 ± 0.10 (n = 11), $p < 0.001$ (permutation test, 100,000 repetitions) for each comparison with the respective wild-type. See Experimental Procedures for details.

[19] in *Drosophila* peripheral nervous system. A monoclonal antibody detected *Cut* in subsets of adPNs and IPNs (~8 for each) and in all vPNs (Figure 2A). The expression pattern appeared similar at 18 hr APF. Costaining with Mz19-Gal4 and various single-cell clones with GH146-Gal4 further narrowed down *Cut*-expressing PN; *Cut*-positive adPNs are likely embryonically born [20] and thus not included in our functional analysis, while DM1 and DM2 IPNs express *Cut*, but DA1, DL3, and DM5 IPNs do not (Figure 4A).

$cut^{-/-}$ adPNs targeted all their normal glomeruli correctly, consistent with their lack of expression (Figure 2B₁). $cut^{-/-}$ IPNs failed to target DM1 (n = 10/12), DM2 (4/12), and VA5 (3/11) (Figure 2B₂). $cut^{-/-}$ vPNs were severely affected, with their cell numbers reduced from 4–6 in wild-type to 2–3 in $cut^{-/-}$ clones. $cut^{-/-}$ vPNs failed to elaborate their dendrites correctly in the AL and mistargeted the SOG (Figure 2B₃). In summary, *cut* is required by a specific subset of IPNs and all vPNs that express *Cut* (Figure 4A; *Cut* expression in VA5 IPNs has not been determined).

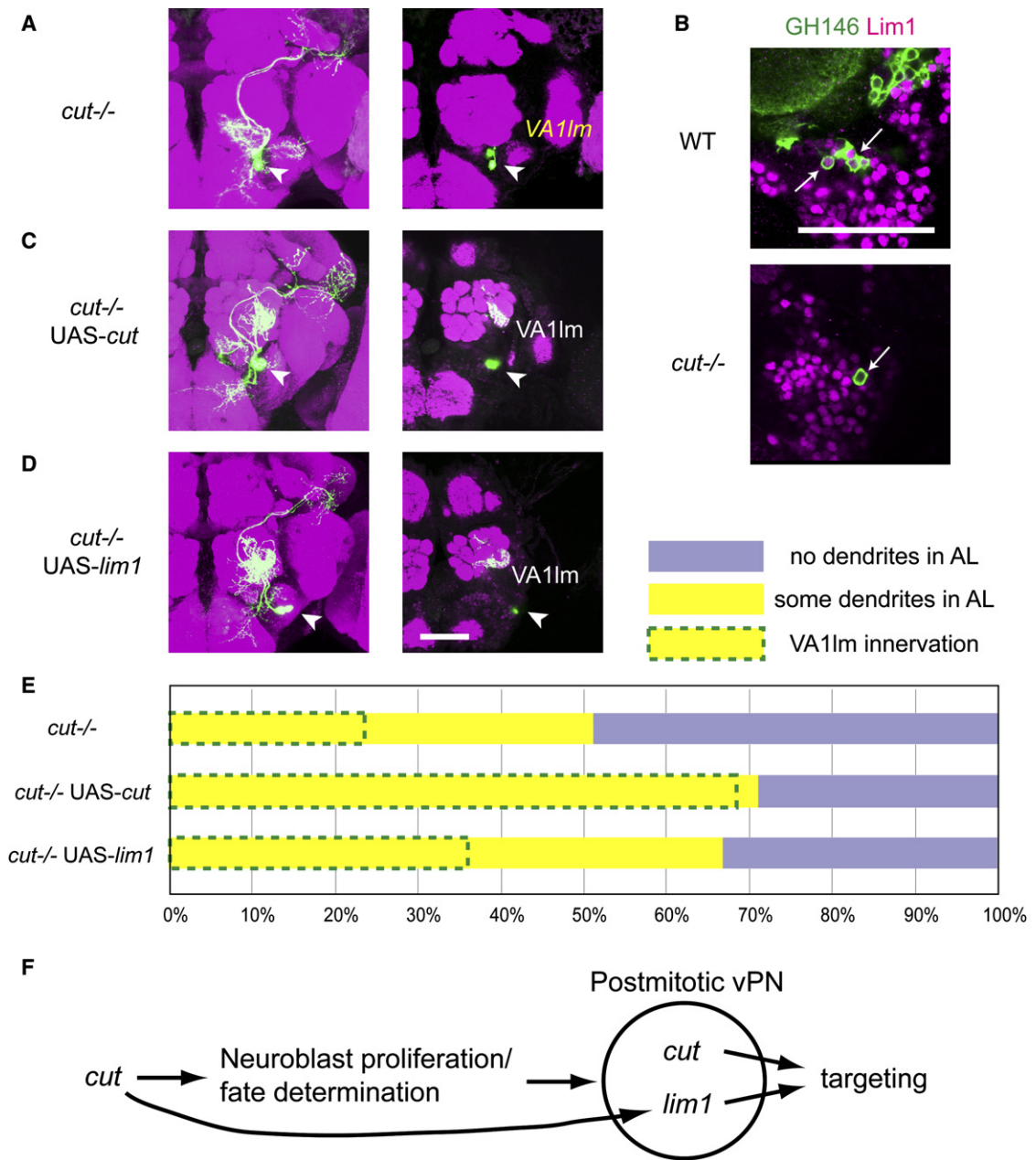


Figure 3. *cut* Functions Both Pre- and Postmitotically in vPN Development and Functions Redundantly with *lim1* in Postmitotic vPNs

(A) *cut*^{-/-} vPNs mistarget a large fraction of dendrites to the SOG and often completely miss the AL.
 (A, C, and D) Left panels are confocal z-projections to show the full extent of targeting, and right panels are single confocal sections to show the anterior AL.
 (B) *cut*^{-/-} vPNs fail to strongly express Lim1. Magenta, anti-Lim1; green, UAS-mCD8GFP driven by GH146-Gal4. A single confocal section is shown.
 (C) Failure of VA1Im innervation by *cut*^{-/-} vPNs is partially rescued by postmitotic expression of a *cut* transgene. The cell number decrease is not rescued.
 (D) Postmitotic expression of a *lim1* transgene partially suppresses the failure of AL innervation and VA1Im innervation of *cut*^{-/-} vPNs. The cell number decrease is not suppressed.
 (E) Quantification of the phenotypes observed in *cut*^{-/-} vPNs and *cut*^{-/-} vPNs expressing a UAS-*cut* or UAS-*lim1* transgene. n = 43 for *cut*^{-/-}, 38 for *cut*^{-/-} UAS-*cut*, and 33 for *cut*^{-/-} UAS-*lim1*.
 (F) A model for functions of *cut* and *lim1* in vPN development. *cut* functions premitotically to regulate vPN neuroblast proliferation and/or cell-fate determination. This includes upregulation of Lim1 expression. In postmitotic vPNs, *cut* and *lim1* function redundantly to regulate dendritic targeting to the AL and then to VA1Im.

cut appears to control global targeting of PN dendrites along mediolateral axis, as indicated by the fact that loss and gain of *cut* in IPNs causes a lateral and medial shift of

dendrites, respectively (Figure 2C₁, top; Figure 2C₂, p < 0.001, see Experimental Procedures). adPNs do not show a *cut* loss-of-function defect, consistent with

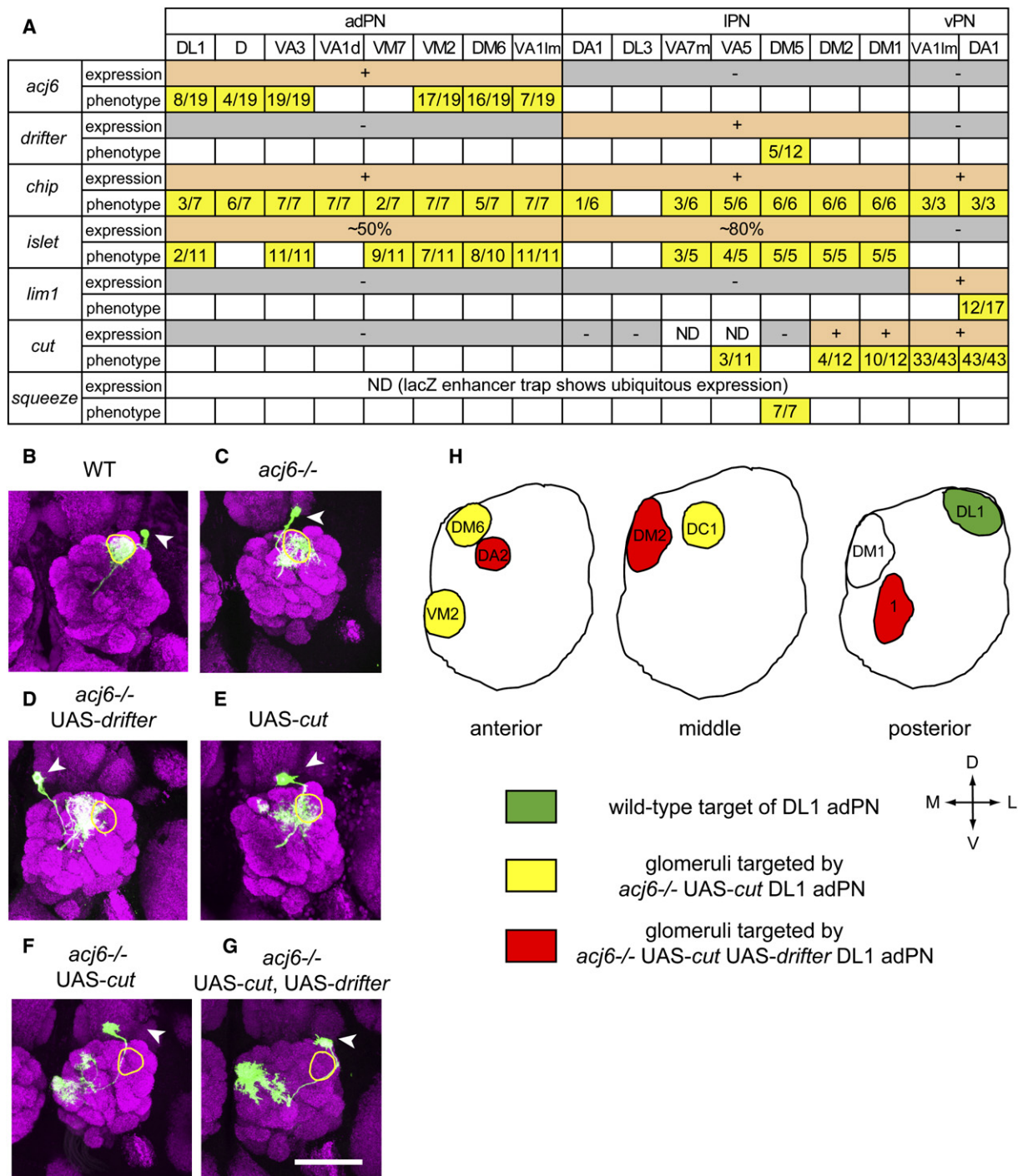


Figure 4. Cooperative and Instructive Effects of Transcription Factors

(A) Summary of expression patterns and dendritic targeting defects for the seven factors discussed in this paper. Fractions in yellow-highlighted boxes represent the number of clones with respective defects/number of clones examined. Empty white boxes in phenotype rows represent correct targeting. +, expressed; -, not expressed; %, the percentage of PN that express the TF. The data for *acj6* and *drifter* are taken from [6]. The data for *squeeze* is presented in Supplemental Data. ND, not determined.

(B-G) Yellow lines outline the DL1 glomerulus, drawn based on careful examination of nc82 staining through confocal stacks. The slight variation of DL1 positions in different images (B-G) reflect slightly different angles by which brains are mounted on slides. Confocal z-projections are shown.

(B) WT DL1 single-cell clone.

(C) Loss of *acj6* causes dendrites to be diffuse in a nondirectional way, but DL1 is still at least partially innervated.

(D) *drifter* misexpression in *acj6*^{-/-} DL1 adPNs cause anterior mistargeting of dendrites [6]. DL1 is not innervated, but in the z-projection shown, it appears innervated.

(E) *cut* misexpression causes the dendrites of DL1 single-cell clones to diffuse in the medial direction, but they still partially innervate DL1.

(F) Simultaneous loss of *acj6* and gain of *cut* cause the dendrites to completely miss DL1 and target in the medial AL.

the lack of expression (Figure 2B₁). Nevertheless, *cut* misexpression in adPNs shifted their dendrites medially (Figure 2C₁, bottom). Interestingly, adPNs misexpressing *cut* usually avoid DM1 and DM2, suggesting that *cut* controls global targeting, rather than simply promoting innervation of these glomeruli.

Postmitotic expression of a *cut* transgene only in labeled *cut*^{-/-} IPNs completely rescued targeting of DM1, DM2, and VA5 (7/7). There were also gain-of-function phenotypes, and DA1 and DL3 innervation was often lacking in these clones (data not shown). Thus, *cut* postmitotically rescues dendritic targeting defects of IPNs that normally express *cut*, whereas postmitotic misexpression in other IPNs disrupts their targeting fidelity.

The vPN rescue phenotype was more complex (Figures 3C and 3E). The cell number decrease was not rescued by postmitotic *cut* expression. However, the targeting defect was partially rescued. 71% of vPN rescue clones examined sent some dendrites to the AL (the rest completely failed to innervate the AL), and 68% innervated VA1Im. This is markedly better than *cut*^{-/-}, in which only 51% entered the AL and 23% innervated VA1Im (Figure 3E). DA1 targeting was not rescued, raising the possibility that the DA1 vPN was never born or correctly specified in these animals.

Relationship of *cut* and *lim1* in vPNs

The *lim1* phenotype in vPNs is a subset of the *cut* phenotype (Figure 4A). We found that Lim1 immunoreactivity in *cut*^{-/-} vPNs was either absent or greatly reduced compared to wild-type (Figure 3B). Therefore, Cut directly or indirectly controls Lim1 expression.

If a major function of Cut in vPNs is to upregulate Lim1, then transgenic *lim1* expression in *cut*^{-/-} vPNs might suppress part of the *cut*^{-/-} phenotype. In *cut*^{-/-} vPNs expressing a *lim1* transgene (Figures 3D and 3E), the reduction of cell number was not suppressed. However, 67% clones innervated the AL (compared to 51% in *cut*^{-/-}). VA1Im innervation was also mildly improved (36% in UAS-*lim1* versus 23% in *cut*^{-/-}). Thus, UAS-*lim1* expression partially suppressed *cut*^{-/-} targeting defects, although not quite as well as UAS-*cut* (Figure 3E). In contrast, UAS-*lim1* expression in *cut*^{-/-} IPNs, which normally do not express Lim1, did not suppress the *cut*^{-/-} targeting defects (data not shown). Therefore, Cut and Lim1 are not simply interchangeable, and the partial suppression of *cut*^{-/-} defects by *lim1* is specific to vPNs.

Although postmitotic expression of *cut* partially rescued the *cut*^{-/-} vPN phenotypes (Figure 3E), it failed to rescue Lim1 expression (data not shown). In addition, postmitotic misexpression of *cut* in adPNs or IPNs did not lead to an ectopic expression of Lim1 (data not shown). Therefore, *cut* is not sufficient to upregulate Lim1 expression in postmitotic neurons. We propose that *cut* functions at two distinct stages of vPN development (Figure 3F). First, *cut* controls the proliferation and/or fate specification of the vPN neuroblast, including

Lim1 expression. Second, *cut* controls dendritic targeting by postmitotic VA1Im vPNs, partially redundantly with *lim1*. This partial redundancy may explain the observation that *lim1*^{-/-} vPNs target VA1Im normally (Figure 1F₃). These pre- and postmitotic functions of *cut* in the same neuronal lineage are reminiscent of its function in peripheral nervous system development [18, 19].

Distinct Functions of Instructive Transcription Factors

If combinations of the TFs identified here instruct PN dendritic targeting, then misexpression or swapping of them might cause predictable changes of targeting specificity. We tested this hypothesis by using the DL1 adPN as a model, because we can unambiguously identify this class based on the time of heat shock to induce clones with GH146-Gal4 [4] (Figure 4B), and GH146-Gal4 is strong enough for single-cell rescue or misexpression experiments [6].

DL1 adPN expresses *Acj6*, an adPN lineage factor [6], but not *Drifter* or *Cut* (Figure 4A). *acj6*^{-/-} DL1 PN typically have diffuse dendrites that always innervate, but are not limited to, DL1 [6] (Figure 4C). *drifter* misexpression alone did not affect their dendritic targeting. However, when loss of *acj6* and gain of *drifter* were combined, the dendrites completely missed DL1 and targeted anterior glomeruli [6] (Figure 4D).

Misexpression of *Cut* alone caused DL1 PNs to target part of DL1 and the vicinity (Figure 4E), similar to *acj6*^{-/-} (Figure 4C). Notably, this diffuse phenotype was directional, because most mistargeted dendrites targeted medially to DL1 (Figure 4E, n = 9).

cut misexpression combined with loss of *acj6* caused severe mistargeting of DL1 adPNs (Figure 4F, n = 15). The dendrites completely missed DL1 and occupied the medial to dorsomedial AL, typically VM2, DM6, and DC1 (n = 9/15, 7/15, and 4/15, respectively; Figure 4H, yellow). Interestingly, these glomeruli are all adPN targets [4, 21] near DM1 and DM2, the two glomeruli that most frequently fail to be innervated by *cut*^{-/-} IPNs (Figure 4A). One interpretation is that loss of *acj6* made the DL1 adPN more sensitive to the instructive information of *cut* to target the medial AL, but the remaining lineage information kept the dendrites within the adPN glomeruli in the area. If this were true, adding a IPN lineage factor *drifter* may bring the dendrites to DM1 or DM2, since this might recreate, based on our partial knowledge of the TF code (Figure 4A), a code for targeting these glomeruli. We thus combined loss of *acj6* and misexpression of *cut* and *drifter* simultaneously in DL1 adPNs. Under this condition, the dendrites again mostly targeted the medial to dorsomedial AL (Figure 4G, n = 11). However, glomerular preferences were strikingly different: they frequently innervated 1, DM2, and DA2 (n = 5/11, 4/11, and 3/11, respectively; Figure 4H, red). Notably, DA2 and DM2 are IPN targets [4, 21].

These results suggest that *cut* and *drifter* have qualitatively different instructive information, with *cut*

(G) Simultaneous loss of *acj6* and gain of *cut* and *drifter* result in targeting of the medial AL.

(H) Positions of glomeruli frequently innervated by the swap experiments (F and G). Note that glomeruli innervated by *acj6*^{-/-} UAS-*cut* DL1 adPN (yellow; an example is shown in [F]) and those targeted by *acj6*^{-/-} UAS-*cut* UAS-*drifter* DL1 adPN (red; an example is shown in [G]) are located adjacently in a similar area but nonoverlapping.

controlling global targeting and *drifter* controlling local glomerular choice according to their lineage.

Discussion

Experiments described here, together with our previous study [6], identified six TFs and a cofactor required for dendritic targeting of specific subsets of 17 classes of *Drosophila* olfactory projection neurons (Figure 4A). Of the six TFs identified here, at least five are expressed in subsets of PNs. Based on the expression data (Figure 4A), we estimate that expression of these six TFs could define 5–11 unique identities (see **Experimental Procedures**). Although we have not identified unique combinations of TFs for all 17 classes studied here, our results suggest that distinct PN classes are at least partially defined by combinatorial expression of TFs that regulate their targeting specificity.

How many TFs are required to specify the dendritic targeting of 17 PN classes? With a binary combinatorial code, 5 factors could specify 2^5 (=32) different states. If different levels of single factors carry different information (e.g., [19]), even fewer factors could be sufficient. However, we have identified six TFs that regulate dendritic targeting specificity of subsets of PN classes, or “specificity TFs,” after testing 14 candidate TFs. Given that there are 694 predicted TFs in the *Drosophila* genome [22], it is almost certain that we have identified only a small fraction of specificity TFs. Thus, the number of specificity TFs is likely much larger than the theoretical minimum.

Redundancy could be a major reason. *cut* and *lim1* in vPNs provide an example. Redundancy could ensure the robustness of wiring, making it tolerant to mutations in specificity TFs. Such tolerance could provide a substrate for evolution, allowing mutations to accumulate without devastating effects on the wiring of preexisting neuronal classes and making it easier for new classes to evolve. Whatever the evolutionary advantages might be, we suggest that many TFs function redundantly and at different levels in a complex hierarchy that cooperatively define neuronal connection specificity.

We find that different TFs regulate different steps of dendritic targeting, some specifying the coarse area (e.g., *cut*), followed by others controlling local glomerular choice within the area (e.g., *drifter* and *acj6*). We previously found that adPNs and IPNs target highly intercalating but nonoverlapping sets of glomeruli [4]. This could be explained now by *acj6* and *drifter* controlling local glomerular choices, enabling adPNs and IPNs to locally segregate into distinct sets of glomeruli. These findings fit well with our recent finding that graded expression of *Sema1a* cell-autonomously controls the initial and coarse targeting of PN dendrites along the dorso-lateral to ventromedial axis [23]. This coarse targeting is likely refined by PN dendrodendritic interactions [24] and ORN-PN interactions [25]. Thus, PN dendrites perform multistep targeting, gradually restricting their dendritic regions. Such multistep targeting could increase the robustness of neuronal wiring, reducing the complexity of decisions at each decision point and minimizing mistakes made by each neuron.

Our results begin to provide insights into the global strategy of how an ensemble of TFs regulates wiring

specificity of a large number of neurons constituting a neural circuit. We envision that the properties we have identified here, such as a redundant TF code and multistep targeting, are generally applicable to the establishment of wiring specificity of other complex neural circuits in nervous systems.

Experimental Procedures

Fly Stocks

In mutant analyses for *islet*, *lim1*, and *cut*, two independent alleles gave indistinguishable phenotypes, and the results were pooled (*islet*, *islet*^{37Aa} and *tup*¹; *lim1*, *lim1*^{E4} and *lim1*^{E3}; *cut*, *cut*^{C145} and *cut*^{db3}). Information for alleles used can be found in the Flybase (<http://flybase.bio.indiana.edu/>).

Clonal and Phenotypic Analysis

MARCM was performed as previously described [6, 7]. Images were obtained with Biorad MRC 1024 and Zeiss LSM 510. Dendritic targeting was scored as defective when innervation to a given glomerulus is either absent, markedly reduced, and/or considerably diffuse.

Immunostaining

Staining and imaging were performed as previously described [6]. The following antibodies were used: rat anti-mCD8 α (Caltag), 1:100; mAb nc82 (a gift from E. Buchner), 1:35; rat anti-Aristaless (a gift from G. Campbell), 1:500; rabbit anti-Pdm-1 (a gift from X. Yang), 1:1000; mAb anti-Cut (DSHB), 1:20; guinea pig anti-Lim1 (a gift from J. Botas), 1:500; rat anti-Islet (a gift from J. Skeath), 1:1000; rabbit anti-Chip (a gift from D. Dorsett), 1:500.

Quantitative Analysis of Dendritic Distributions along the Medial-Lateral Axis

This was done essentially as described in a separate manuscript [23]. A custom-made MATLAB program was used. In short, dendritic termini in the AL were manually selected from confocal z-projections, and the medial-lateral axis was manually drawn. Along the axis, the AL was binned into 10 bins and the relative amount of dendrites (green labeling) in each bin was calculated. Each brain was normalized so that the total amount of dendrites from each clone was 1. The mean distribution from multiple clones of each genotype was plotted, and the mean of mean positions was calculated for each genotype (dotted lines). Statistics are by permutation tests with 100,000 repetitions.

An Estimate of the Number of States Defined by Expression of the Identified TFs

With the TFs identified here, how many different expression profiles can we define? Because we have not determined the precise PN classes that express Islet or Sqz, this has to be an estimate with a range. With the matrix of (Acj6, Drifter, Islet, Lim1, Cut), we can define (+, -, +, -, -) and (+, -, -, -, -) for adPNs (+ for expression, - for lack of expression). For IPNs, (-, +, +, -, -) and (-, +, +, -, +) can be defined. In addition, depending on the extent of overlap and segregation of expression patterns of Islet and Cut, (-, +, -, -) and (-, +, -, +) could be additionally defined. If Sqz is expressed in a specific subset of IPNs, up to four additional states could be defined. vPNs can be defined as (-, -, -, +, +). Therefore, based on expression patterns of the 6 TFs described, we can define 5 to 11 groups of the 17 PN classes.

Supplemental Data

Supplemental Data include one figure and Results and can be found with this article online at <http://www.current-biology.com/cgi/content/full/17/3/278/DC1/>.

Acknowledgments

We thank J. Botas, E. Buchner, G. Campbell, D. Dorsett, J. Skeath, J. Thomas, X. Yang, and the Developmental Studies Hybridoma Bank for antibodies; J.P. Couso, J. Curtiss, C. Doe, E. Giniger, W. Grueber, Y.N. Jan, T. Kojima, K. Melnattur, J. Nambu, J. Thomas,

S. Thor, and the Bloomington Stock Center for fly stocks; and G.S.X.E. Jefferis and members of the Luo lab for comments on the manuscript. This work was supported by an NIH grant (R01-DC 005982) to L.L. L.L. is an investigator of Howard Hughes Medical Institute.

Received: October 23, 2006

Revised: November 21, 2006

Accepted: November 24, 2006

Published: February 5, 2007

References

1. Dickson, B.J. (2002). Molecular mechanisms of axon guidance. *Science* 298, 1959–1964.
2. Jan, Y.N., and Jan, L.Y. (2003). The control of dendrite development. *Neuron* 40, 229–242.
3. Komiyama, T., and Luo, L. (2006). Development of wiring specificity in the olfactory system. *Curr. Opin. Neurobiol.* 16, 67–73.
4. Jefferis, G.S.X.E., Marin, E.C., Stocker, R.F., and Luo, L. (2001). Target neuron prespecification in the olfactory map of *Drosophila*. *Nature* 414, 204–208.
5. Jefferis, G.S.X.E., Vyas, R.M., Berdnik, D., Ramaekers, A., Stocker, R.F., Tanaka, N., Ito, K., and Luo, L. (2004). Developmental origin of wiring specificity in the olfactory system of *Drosophila*. *Development* 131, 117–130.
6. Komiyama, T., Johnson, W.A., Luo, L., and Jefferis, G.S.X.E. (2003). From lineage to wiring specificity. POU domain transcription factors control precise connections of *Drosophila* olfactory projection neurons. *Cell* 112, 157–167.
7. Lee, T., and Luo, L. (1999). Mosaic analysis with a repressible cell marker for studies of gene function in neuronal morphogenesis. *Neuron* 22, 451–461.
8. Shirasaki, R., and Pfaff, S.L. (2002). Transcriptional codes and the control of neuronal identity. *Annu. Rev. Neurosci.* 25, 251–281.
9. Bach, I. (2000). The LIM domain: regulation by association. *Mech. Dev.* 91, 5–17.
10. Morcillo, P., Rosen, C., Baylies, M.K., and Dorsett, D. (1997). Chip, a widely expressed chromosomal protein required for segmentation and activity of a remote wing margin enhancer in *Drosophila*. *Genes Dev.* 11, 2729–2740.
11. van Meyel, D.J., O'Keefe, D.D., Jurata, L.W., Thor, S., Gill, G.N., and Thomas, J.B. (1999). Chip and apterous physically interact to form a functional complex during *Drosophila* development. *Mol. Cell* 4, 259–265.
12. Marin, E.C., Jefferis, G.S.X.E., Komiyama, T., Zhu, H., and Luo, L. (2002). Representation of the glomerular olfactory map in the *Drosophila* brain. *Cell* 109, 243–255.
13. Broihier, H.T., and Skeath, J.B. (2002). *Drosophila* homeodomain protein dHb9 directs neuronal fate via crossrepressive and cell-nonautonomous mechanisms. *Neuron* 35, 39–50.
14. Lilly, B., O'Keefe, D.D., Thomas, J.B., and Botas, J. (1999). The LIM homeodomain protein dLim1 defines a subclass of neurons within the embryonic ventral nerve cord of *Drosophila*. *Mech. Dev.* 88, 195–205.
15. Pueyo, J.I., and Couso, J.P. (2004). Chip-mediated partnerships of the homeodomain proteins Bar and Aristaless with the LIM-HOM proteins Apterous and Lim1 regulate distal leg development. *Development* 131, 3107–3120.
16. Torigoi, E., Bennani-Baiti, I.M., Rosen, C., Gonzalez, K., Morcillo, P., Ptashne, M., and Dorsett, D. (2000). Chip interacts with diverse homeodomain proteins and potentiates bicoid activity in vivo. *Proc. Natl. Acad. Sci. USA* 97, 2686–2691.
17. Romain, P., Khechumian, R., Khechumian, K., Arbogast, N., Ackermann, C., and Heitzler, P. (2000). Interactions between chip and the achaete/scute-daughterless heterodimers are required for panner-driven proneural patterning. *Mol. Cell* 6, 781–790.
18. Bodmer, R., Barbel, S., Sheperd, S., Jack, J.W., Jan, L.Y., and Jan, Y.N. (1987). Transformation of sensory organs by mutations of the cut locus of *D. melanogaster*. *Cell* 51, 293–307.
19. Grueber, W.B., Jan, L.Y., and Jan, Y.N. (2003). Different levels of the homeodomain protein cut regulate distinct dendrite branching patterns of *Drosophila* multidendritic neurons. *Cell* 112, 805–818.
20. Marin, E.C., Watts, R.J., Tanaka, N.K., Ito, K., and Luo, L. (2005). Developmentally programmed remodeling of the *Drosophila* olfactory circuit. *Development* 132, 725–737.
21. Wong, A.M., Wang, J.W., and Axel, R. (2002). Spatial representation of the glomerular map in the *Drosophila* protocerebrum. *Cell* 109, 229–241.
22. Adams, M.D., Celniker, S.E., Holt, R.A., Evans, C.A., Gocayne, J.D., Amanatides, P.G., Scherer, S.E., Li, P.W., Hoskins, R.A., Galle, R.F., et al. (2000). The genome sequence of *Drosophila melanogaster*. *Science* 287, 2185–2195.
23. Komiyama, T., Sweeney, L.B., Schuldiner, O., Garcia, K.C., and Luo, L. (2007). Graded expression of Semaphorin-1a cell-autonomously directs dendritic targeting of olfactory projection neurons. *Cell* 128, 399–410.
24. Zhu, H., and Luo, L. (2004). Diverse functions of N-cadherin in dendritic and axonal terminal arborization of olfactory projection neurons. *Neuron* 42, 63–75.
25. Zhu, H., Hummel, T., Clemens, J.C., Berdnik, D., Zipursky, S.L., and Luo, L. (2006). Dendritic patterning by Dscam and synaptic partner matching in the *Drosophila* antennal lobe. *Nat. Neurosci.* 9, 349–355.